42nd AIAA Aerospace Sciences Meeting and Exhibit
5-8 January 2004, Reno, Nevada

AIAA 2004-1137

ANALYSIS AND DESIGN OF RECTANGULAR-CROSS-SECTION NOZZLES FOR SCRAMJET ENGINE TESTING

Richard L. Gaffney, Jr.*
John J. Korte†

NASA Langley Research Center, Hampton, Virginia.

ABSTRACT

The flow in the square-cross-section Mach-6 nozzle used in the NASA Langley Research Center Arc-Heated Scramjet Test Facility has been analyzed using three-dimensional viscous CFD methods. The primary cause of the non-uniform flow exiting the nozzle is identified as cross-flow pressure gradients imposed on wall boundary layers. The cross-flow pressure gradients cause the boundary layer to roll up into counter-rotating vortex pairs on each of the four sides of the nozzle. These four vortex pairs produce significant non-uniformity in the nozzle-exit flow. In order to improve the quality of the test flow in the facility, two alternative nozzle designs (one axisymmetric and one rectangular with a 2-D contour) have been investigated. While the axisymmetric design produced the most uniform flow, the 2-D design also produced very good flow. The 2-D design was selected for further refinement, resulting in a new nozzle design which has been constructed and awaits calibration.

INTRODUCTION

The Arc-Heated Scramjet Test Facility (AHSTF) is a high-enthalpy wind tunnel used to test supersonic combustion ramjet (scramjet) engines. The high total enthalpies needed for engine tests are achieved by heating a portion of the test gas with an electric arc and mixing this with unheated by-pass air to obtain the desired total enthalpy. The heated gas is expanded to test conditions through a facility nozzle where it enters the test cabin as a free jet. This facility produces enthalpies which correspond to vehicle flight Mach numbers of 4.7 to 8.[1]

From the early 1980's until 2002 a Mach-6 square-cross-section nozzle has been used in the AHSTF. This nozzle expands the flow equally along each of its four identically-contoured sides. It is 61.811 inches long from the throat to the exit, has a throat height of 1.144 inches and an exit height of 10.892 inches. This gives an exit-area to throat-area ratio of 90.649. The contour of the subsonic portion of the throat is composed of a circular arc of radius 8.5 inches. The contour of the nozzle is plotted in figure 1.

The nozzle was designed by inscribing a square inside the circular throat of an axisymmetric method-of-characteristics (MOC) design and then tracing streamlines from that square to the nozzle exit. The traced streamlines give square cross-sections at the starting plane, the plane of the contour inflection and at the nozzle exit. The contour at all the other axial locations was adjusted so that every cross-section was square.[2] The final step was to apply a correction to the contour based on the results of an integral boundary-layer calculation.[3]

The rectangular cross-section design was required so that the boundary layer from the facility nozzle could be used to simulate the boundary layer on the forebody of a hypersonic vehicle for scramjet engine testing.[4] The square cross-section was chosen because it has a smaller surface area (and heat loss) in the throat region than a rectangular shaped nozzle. It was also thought that the square cross-section would reduce the effect of boundary layer growth in the throat region.[5]

Unfortunately, the flow at the exit of this nozzle is non-uniform[5,6] which can adversely affect tests being conducted in the facility. The goal of the current work is three-fold; to identify the cause of the non-uniformities, to examine alternative nozzle designs, and to design a new Mach-6 nozzle.

*Senior Member AIAA, Aerospace Engineer, Hypersonic Airbreathing Propulsion Branch
†Associate Fellow AIAA, Senior Research Scientist, Multidisciplinary Optimization Branch

NOZZLE ANALYSIS

Before a new nozzle is designed, it is important to understand the flow physics of the square-cross-section nozzle in order to avoid the flow structures which produce the non-uniform flow. This has been accomplished through the use of a 3-D viscous CFD calculation. Flow conditions for the calculation matched a Mach-7 flight-enthalpy condition taken from a 1998 calibration of the nozzle.[6] The nozzle plenum conditions were

$$P_t = 410 \text{ psi}$$
$$T_t = 3760 \text{ °R}$$

where P_t is the total pressure and T_t is the total temperature. The species in the test gas[7] are listed in the table below.

Species	Mass Fraction	Mole Fraction
N_2	0.7460	0.7710
O_2	0.2188	0.1980
NO	0.0228	0.0220
Ar	0.0124	0.0090

Table 1: Test Gas Mass and Mole Fractions

The calculation was accomplished using the VULCAN CFD program[8] for one quarter of the geometry (taking advantage of nozzle symmetries). The grid dimensions were 321 in the axial direction and 65 in each of the two cross-flow directions. Points were clustered near the solid walls and in the throat region. The solution was generated by solving the thin-layer Navier-Stokes equations using Roe's flux-difference-splitting scheme and an elliptic solution algorithm. Wall functions were used with the k-ω turbulence model to reduce the number of grid points required in the near-wall region. The thermodynamic state of the gas was determined from curve fits computed for gases in vibrational equilibrium. The inflow boundary was set to uniform flow, the supersonic outflow boundary was extrapolated and the nozzle surface was set to a constant wall temperature of 600 K. The L2 norm of the solution residual was converged 10 orders of magnitude.

Mach number contours in the nozzle exit plane are shown in Figure 2 (mirrored for clarity). Non-uniform flow has developed near the wall in the middle of each of the four sides. The cross-flow velocity-vector and streamline plot of the upper right quadrant of the exit (Figure 3) reveals counter rotating vortex pairs near the middle of each wall. Figure 4 (also mirrored) shows pressure contours in the nozzle exit plane. The lowest pressures are in the corners and the higher pressures are in the center. The pressure varies 25% across the exit plane where the variation is measured by the percent difference, defined as

$$\% \text{ difference} = \frac{|max - min|}{\frac{1}{2}|max + min|} \times 100$$

Within the core flow, a square 6.6 inches on a side, the pressure varies by 16% and the Mach number varies by 2.6%. Figures 5 and 6 show Mach number and pressure profiles in a vertical symmetry plane at the nozzle exit. It is seen that a smaller core flow size would have more uniform flow.

Previous researchers,[9] have found that nozzles with 2-D contours have transverse pressure gradients which adversely affect the side wall boundary layers. This was verified in the current work by repeating the CFD calculation assuming inviscid flow. This calculation was done using a grid with the same grid dimensions and axial point distribution as the viscous grid but with evenly spaced grid points in the two cross-flow directions. The solution residual was reduced 11 orders of magnitude for the calculation. Figure 7 shows the Mach contours in the nozzle exit plane for the inviscid calculation. The flow structure is very different from the viscous calculation. The velocity vectors and streamlines in the exit plane (Figure 8) show no evidence of the vortices seen in the turbulent solution. This confirms that the primary problem with the non-uniform flow is an interaction of the inviscid core flow with the wall boundary layer.

An examination of Figure 9, which shows pressure contours in a vertical symmetry plane, reveals that in the expansion region of the nozzle the pressure gradient is parallel to the flow direction. However, in the turning section of the nozzle, the pressure gradient is at an angle with respect to the flow. This means that there is a cross-flow component of the pressure gradient. This is illustrated in the inset of Figure 9 which shows the pressure distribution taken along a vertical line. At this axial location, the pressure is high near the nozzle surface and low at the nozzle centerline. This causes the streamlines to curve away from the high pressure towards the low pressure region. In the boundary layer, the fluid closer to the wall has lower momentum and turns more than the higher-momentum fluid closer to the edge of the boundary layer. This produces streamwise vorticity and leads to cross-flow separation. In a supersonic nozzle, the flow above and below the centerline curve towards the centerline (lowest pressure) and separate into counter-rotating vortex pairs where they meet. In the current nozzle, which expands the flow both vertically and horizontally, vor-

tex pairs are generated on each of the four walls.

ALTERNATIVE DESIGNS

Since the flow non-uniformity in the square-cross-section nozzle is the result of cross-flow pressure gradients imposed on the wall boundary layers, a new nozzle design should mitigate this effect. With this criterion, an axisymmetric nozzle is the most logical choice. In axisymmetric nozzles, the pressure gradient is always perpendicular to the surface so vortices never form. Axisymmetric nozzles also have an advantage over other shapes for high enthalpy flows because they present the minimum surface area to the flow, thus minimizing cooling requirements.

While axisymmetric nozzles may produce the most uniform flow, they are not necessarily the best solution for scramjet engine testing. In an airframe-integrated scramjet, an engine may be composed of multiple flow-paths (modules) which are adjacent to one another. Modules with rectangular cross sections are often used because they stack side-by-side without wasting volume. Facility nozzles with a shape similar to the inlet capture area (rectangular) are the most compatible with this type of design. In addition, it is desirable to be able to mount the forebody/engine in a position to ingest the facility-nozzle boundary layer which simulates the boundary layer which would have developed on an airframe-integrated scramjet with a longer forebody. (Often times, the forebody of an airframe-integrated scramjet is truncated to make it fit in the facility.)

With these thoughts in mind, two nozzles were designed and their merits compared. The first nozzle design was an axisymmetric nozzle and the second was a 3-D nozzle with a 2-D contour (contoured upper and lower surfaces and flat side walls).

Design Method

The method-of-characteristics (MOC) method of Sivells[10] was used to design the two nozzle contours. This method computes the contour from a centerline Mach number distribution. Sivells divides the centerline distribution into three parts: the throat region which is specified by a 4^{th} order polynomial, a radial flow region, and a downstream region which is specified by a 5^{th} order polynomial. The coefficients of the polynomials are set such that the second derivative of the axial velocity is continuous throughout and is zero in the uniform flow region. The subsonic portion of the throat region is computed using a Gaussian curve.

Sivells' program is for a constant γ (ratio of specific heats) flow which does not apply to high-enthalpy hypersonic nozzles which can have significant effects due to γ variation. Korte[11] has developed a procedure to account for γ variation by taking advantage of the radial flow region in Sivells' program. Korte's procedure is to run Sivells' code twice, once using a value of γ which is characteristic of the high temperature flow in the throat region and a second time using a γ associated with the much cooler exit flow. Korte then blends the contour upstream of the radial region, generated with the high-temperature γ, and the contour downstream of the radial region, generated with the low-temperature γ, by matching the two contours in the linear segment of the radial-flow region.

Viscous effects were included in the design method through an iterative procedure using Korte's method and the multi-dimensional viscous CFD code VULCAN. In the design procedure the MOC exit area was specified larger than that was needed for the inviscid design Mach number. The CFD code was then run using the MOC contour and the exit Mach number checked. If the CFD exit Mach number did not match the design Mach number, the MOC code was re-run using an adjusted exit area. The CFD was then re-run and the process repeated until the CFD computed exit Mach number matched the design Mach number.

Normally, a nozzle designed in this manner would be truncated in order to maximize flow uniformity and core size. (Since MOC designs have a zero slope at the nozzle exit there is a point in the nozzle where further boundary layer growth reduces the core size and recompresses the flow.) However, since the goal of the alternative design study was simply to scope out possible designs, this last step was not done.

In succinct form, the design steps are:

1. For the design total conditions, compute γ at Mach 1 and at the desired nozzle exit Mach number.
2. Use the MOC code to compute the contour which gives the desired throat area using the γ computed for the throat region.
3. Compute or estimate the area ratio needed to achieve the desired exit Mach number.
4. Use the MOC code to compute the downstream portion of the nozzle using the γ computed for the nozzle exit.
5. Shift the downstream contour so that it matches the upstream contour in the conical expansion section.

6. Compute the subsonic portion of the nozzle contour.
7. Compute the viscous flow field using the VULCAN CFD code.
8. Check exit Mach number and profile. If the design is unacceptable, adjust the exit area and return to step 4.

While the inviscid exit-area to throat-area ratio for the design conditions is 73.4, the existing square-cross-section nozzle, which has already been corrected for a boundary layer, has an area ratio of 90.6. This number was used as the starting value for step 3 for both alternative designs.

Design And Evaluation Conditions

The design conditions for the two alternative nozzle designs were the same as those used to evaluate the square-cross-section nozzle. This includes the total conditions, gas mixture (Table 1) and the surface temperature.

One of the concerns which was considered during the evaluation process was how the nozzles perform in off-design conditions. Axisymmetric nozzles will focus uncanceled waves on the centerline whereas 2-D nozzles tend to focus uncanceled waves on the symmetry plane between the two contoured surfaces. In order to evaluate off-design performance, two off-design conditions were also investigated for the two alternative designs. The off-design conditions were also taken from the recent Mach-6 nozzle calibration.[6] They represent a Mach-5 and a Mach-6 flight-enthalpy. The Mach-6 flight-enthalpy conditions are:

$$P_t = 495 \text{ psi}$$
$$T_t = 2915 \text{ °R}$$

The chemical composition is the same as that given in Table 1. The Mach-5 flight-enthalpy conditions are:

$$P_t = 400 \text{ psi}$$
$$T_t = 2460 \text{ °R}$$

The species mass/mole fractions in the test gas differ from the previous two conditions and are:

Species	Mass Fraction	Mole Fraction
N_2	0.7519	0.7770
O_2	0.2233	0.2020
NO	0.0124	0.0120
Ar	0.0124	0.0090

Table 2: Mach-5 Flight-Enthalpy Off-Design Test Gas Mass and Mole Fractions

Axisymmetric Nozzle

The first nozzle is the axisymmetric design. The throat radius is 0.645 inches and the exit radius is 6.182 inches. The nozzle is 82.83 inches long from the throat to the nozzle exit. The contour for the nozzle is shown in Figure 10. The grid used in the CFD calculation had 201 points in the axial direction and 65 points in the radial direction with points clustered near the throat and at the surface. The solutions were converged 8 to 10 orders of magnitude. The on-design (Mach-7 flight-enthalpy) Mach number profile at the nozzle exit is shown in Figure 11. The Mach number distribution at the exit is very uniform, varying between 6.033 and 6.048 in the core (a 0.24% variation). The pressure in the core is also very uniform as seen in Figure 12. The pressure varies between 0.1863 and 0.1892 psi (a 1.5% variation). This design provides a core region about 9.2 inches in diameter.

The Mach number and pressure profiles at the nozzle exit for the Mach-5-flight-enthalpy off-design condition are reasonably uniform with the Mach number varying between 6.245 and 6.307 and the pressure varying between 0.1660 and 0.1763 psi. (See Figures 13 and 14). This gives a 1.0% variation of Mach number in the core region and a 6.0% variation in pressure. The Mach number and pressure profiles at the nozzle exit for the Mach-6-flight-enthalpy off-design condition are shown in Figures 15 and 16. Within the core flow the Mach number varies between 6.180 and 6.224 (a 0.70% variation) and the pressure varies between 0.2104 and 0.2196 psi (a 4.3% variation).

2-D Contour Nozzle

The second nozzle has a two-dimensional contour and a square exit. The throat height is 0.1194 inches and the exit height (and nozzle width) is 10.958 inches. The nozzle is 72.12 inches long from the throat to the nozzle exit. The contour for the nozzle is shown in Figure 17. The grid had 201 points in the axial direction and 65 points in the two cross-flow directions. The solutions were converged from 8 to 10 orders of magnitude.

Figure 18 shows the Mach number contours for the on-design (Mach-7 flight-enthalpy) case at the nozzle exit plane. As expected, there are only two pairs of vortices, one pair on each planar side wall. This is also seen in the cross-flow velocity vector and streamline plot of Figure 19. The two pair of vortices create some non-uniformity in the pressure field at the nozzle exit as seen in Figure 20. The

percent difference in pressure across the whole exit plane is 6% while it varies 4.6% within a 7.5 inch square core region. The Mach number varies 0.82% within the core region. Figures 21 and 22 show the Mach number and pressure profiles along the vertical and horizontal symmetry planes at the nozzle exit.

Interestingly, the pressure and Mach number variation for the two off-design cases are slightly less than for the on-design case. (These designs were not optimized.) Contours for the Mach number and pressure at the nozzle exit are shown in Figures 23 and 24 for the Mach-5 flight-enthalpy case. Horizontal and vertical profiles for these properties are shown in Figures 25 and 26. These same plots for the Mach-6 flight-enthalpy case are shown in Figures 27 through 30. The pressure varies across the nozzle exit by 5.1% for the Mach-5 flight-enthalpy case and 5.0% for the Mach-6 flight-enthalpy case. Within a smaller core region these numbers are reduced to 4.5% and 3.0%, respectively. Within the core region the Mach number varies by 0.7% for the Mach-5 case and 0.5% for the Mach-6 case.

Nozzle Comparisons

The two alternative Mach-6 nozzles produce fairly uniform flow for the on-design Mach-7 flight-enthalpy conditions. Tables 3 and 4 summarize the computational results for these two nozzles and the existing square-cross-section nozzle.

Nozzle	Range	% Difference
Square	5.902 - 6.058	2.61
Axisym.	6.033 - 6.048	0.24
2-D	5.976 - 6.025	0.82

Table 3: Core Mach Number Variation In Nozzles, Mach-7 Flight-Enthalpy

Nozzle	Range	% Difference
Square	0.1836 - 0.2160	16.2
Axisym.	0.1863 - 0.1892	1.54
2-D	0.1904 - 0.1994	4.62

Table 4: Core Pressure Variation In Nozzles (psi), Mach-7 Flight-Enthalpy

The axisymmetric design is clearly the best in terms of flow uniformity. It has an order of magnitude less variation in both Mach number and pressure than the existing square-cross-section nozzle and a factor of 3 or so less variation than the 2-D nozzle. It also has a larger core size, 9.2 inches in diameter (66.48 in.^{2}) vs. a 7.5 in. square (56.25 in.^{2}) for the 2-D nozzle and a 6.6 in. square (43.56 in.^{2}) for the existing square-cross-section nozzle. While the 2-D contour nozzle is not as uniform as the axisymmetric nozzle, it still has a larger, more uniform core (3 times less variation) than the existing square-cross-section nozzle.

Turning now to off-design performance, results from the Mach-5 flight-enthalpy condition are summarized in Tables 5 and 6.

Nozzle	Range	% Difference
Axisym.	6.245 - 6.307	1.00
2-D	6.225 - 6.271	0.73

Table 5: Core Mach Number Variation In Nozzles - Mach-5 Enthalpy

Nozzle	Range	% Difference
Axisym.	0.1660 - 0.1763	6.05
2-D	0.1715 - 0.1794	4.50

Table 6: Core Pressure Variation In Nozzles (psi), Mach-5 Flight-Enthalpy

As expected, non-uniformity in the exit flow has increased for the axisymmetric nozzle due to uncanceled waves. Both the Mach number and pressure variations changed by a factor of 4. The 2-D nozzle, on the other hand, produces flow which is more uniform than the on-design case. The pressure variation changed by a factor of 1.03 while the Mach number variation changed by a factor of 1.12.

Results from the Mach-6 flight-enthalpy off-design condition are similar and are summarized in Tables 7 and 8.

Nozzle	Range	% Difference
Axisym.	6.180 - 6.224	0.70
2-D	6.160 - 6.185	0.50

Table 7: Core Mach Number Variation In Nozzles, Mach-6 Flight-Enthalpy

Nozzle	Range	% Difference
Axisym.	0.2104 - 0.2196	4.29
2-D	0.2181 - 0.2248	2.99

Table 8: Core Pressure Variation In Nozzles (psi), Mach-6 Flight-Enthalpy

Again, the flow from the axisymmetric nozzle is less uniform at these conditions than for the on-design conditions while the 2-D contour produces more uniform flow. For the axisymmetric nozzle, the Mach number and pressure variations changed by a factor of almost 3. For the 2-D nozzle the Mach number and pressure variations changed by a factor of about 1.6.

Overall, the axisymmetric design had the largest core and provided the most uniform flow of the two designs for on-design conditions while the 2-D contour nozzle proved to be more robust (changed less in uniformity) when operating at off-design conditions. Both nozzles produced considerably more uniform flow than the existing square-cross-section nozzle.

NEW MACH-6 DESIGN

Once the problems with the existing Mach-6 nozzle were understood, and alternative nozzles investigated, a decision was made to build a new facility nozzle. Although an axisymmetric nozzle gives the most uniform flow, a nozzle with a 2-D contour was chosen for the new design in order to retain the possible use of the nozzle boundary layer. The decision was also made to reduce the throat (and exit) area of the new nozzle in order to increase the maximum test pressure available in the facility. The exit area of the nozzle was specified as a square with a 10 inch side. The design conditions for the new nozzle were

$$P_t = 520 \text{ psi}$$
$$T_t = 3887.1 \text{ °R}$$

Species	Mass Fraction	Mole Fraction
N_2	0.7450	0.770
O_2	0.2188	0.198
NO	0.0238	0.023
Ar	0.0124	0.009

Table 10: Test Gas Mass and Mole Fractions

The design wall temperature was 500.0 K.

The new Mach-6 nozzle was designed using the same procedure as previously specified with the exception that the final design was truncated in order to optimize core size and flow uniformity. Twenty-six designs were examined, varying throat radius of curvature, surface slope at the contour inflection point and nozzle area ratio. The final design is 70 inches from the throat to the nozzle exit (truncated from 80 inches), has a throat height of 0.106 inches, and is a constant 10 inches wide with a square exit area. The subsonic portion of the throat contour is defined as a Gaussian curve with a radius of curvature equal to 100 times the throat half height. The contour is plotted in Figure 31. The flow in the new nozzle was analyzed using 3-D, viscous, CFD methods for one quarter of the domain. The grid used in the calculation had 417 points in the axial direction and 65 points in the two cross-flow directions. Points were clustered near the throat and the surface. The solution was converged 8 orders of magnitude.

Mach number contours in the nozzle exit plane are shown in Figure 32 (mirrored for clarity). The boundary layer bulges slightly on each of the two side walls due to the vortex pair on these two walls. The velocity vector and streamline plot of the upper right quadrant of the nozzle exit (Figure 33) reveals a weak counter-rotating vortex pair near the middle of the side wall. Figure 34 (also mirrored) shows pressure contours in the nozzle exit plane. The highest pressures are in the corners and the lowest pressures are near the center of the two side walls (where the vortices are located). This differs from the 2-D alternative nozzle (Figure 20) where the highest pressures were near the middle of the upper and lower surfaces. This difference is the result of truncating the new nozzle at a location where the pressure waves are at a different location. In the new nozzle the pressure varies a maximum of 3.7% across the exit plane. Within a core flow box, 7.5 inches wide and 6.0 inches tall, the pressure varies by 1.7% and the Mach number varies by 0.5%. Figures 35 and 36 show Mach number and pressure profiles in the vertical and horizontal symmetry planes at the nozzle exit.

SUMMARY AND CONCLUDING REMARKS

After analyzing the flow in the existing square-cross-section nozzle and determining that cross-flow pressure gradients were the cause of flow non-uniformities, two new Mach-6 nozzles were investigated for the AHSTF at a Mach-7 flight-enthalpy condition. The first design was axisymmetric and the second was a 2-D contour with a square exit. While the axisymmetric nozzle had the most uniform flow at the on-design condition, both nozzles produced significantly better flow than the existing square-cross-section nozzle. While the 2-D nozzle had a slightly smaller core size, the Mach number and pressure varied less at off-design conditions.

Since the 2-D nozzle produced acceptably uniform flow, it was chosen for further refinement, leading to a new Mach-6 design. The new nozzle is slightly smaller in throat and exit area than the existing square-cross-section nozzle, allowing for an increase in test pressure. Although it is smaller in size, the core size is slightly larger (45 in.^{2} vs. 43.56 in.^{2}) than the existing nozzle. It also has an order of magnitude less variation in pressure and a factor of 5 less variation in Mach number. In addition, the pressure variation across the whole exit is only 3.7%, an important factor when using the nozzle boundary layer to simulate boundary layer growth on a vehicle fore-

body.

The new Mach-6 nozzle was constructed in 2002 and has been installed in the AHSTF. Water cooling manifolds are currently being installed in the facility and the nozzle is scheduled to be calibrated in 2004.

REFERENCES

[1] R. W. Guy, R. C. Rogers, R. L. Puster, K. E. Rock and G. L. Diskin, "The NASA Langley Scramjet Test Complex," AIAA paper 96-3243, July, 1996.

[2] Rizkalla, O., "Inviscid Design and Analysis of Square Supersonic Nozzles," GASL TR 304, December, 1988.

[3] Castrogiovanni, Tony, Private Communication, December, 2003.

[4] Henry, J. R. and Anderson, G. Y., "Design Considerations for the Airframe-Integrated Scramjet," NASA TM X-2895, 1973.

[5] Thomas, S. R., Voland, R. T., and Guy, R. W., "Test Flow Calibration Study of the Langley Arc-Heated Scramjet Test Facility," AIAA paper 87-2165, June, 1987.

[6] Witte, D. W., Irby, R. G., Auslender, A. H., and Rock, K. E., "1998 Calibration of the Mach 4.7 and Mach 6 Arc-Heated Scramjet Test Facility Nozzles," NASA TM in preparation.

[7] Cabell, Karen, Private Communication, January, 2000.

[8] White, J. A. and Morrison, J. H., "A Pseudo-Temporal Multi-Grid Relaxation Scheme for Solving the Parabolized Navier-Stokes Equations," AIAA paper 99-3360, June, 1999.

[9] Owen, J. M. and Sherman, F. S., "Design and Testing of a Mach 4 Axially Symmetric Nozzle for Rarefied Gas Flows," Rept. HE-150-104, Institute of Engineering Research, University of California, Berkeley, California, July, 1952.

[10] Sivells, J. C., "Aerodynamic Design of Axisymmetric Hypersonic Wind-Tunnel Nozzles," Journal of Spacecraft, Vol. 7, No. 11, pp. 1292-1299, November 1970.

[11] Korte, J. J., "Inviscid Design of Hypersonic Wind Tunnel Nozzles for a Real Gas," AIAA paper 2000-0677, January, 2000.

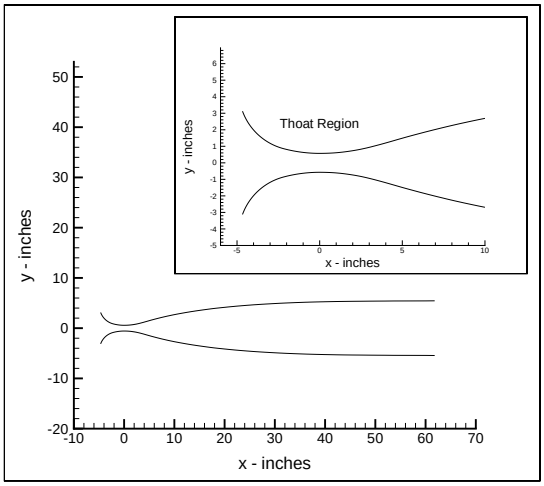

Figure 1: Mach-6 Square-Cross-Section Nozzle Contour

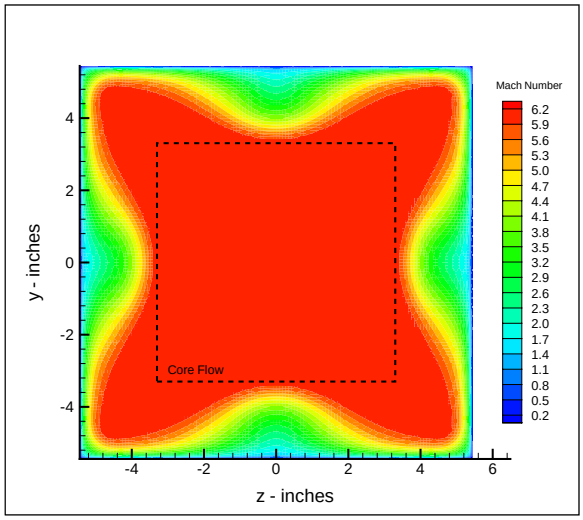

Figure 2: Mach Number Contours at the Exit of the Square-Cross-Section Nozzle

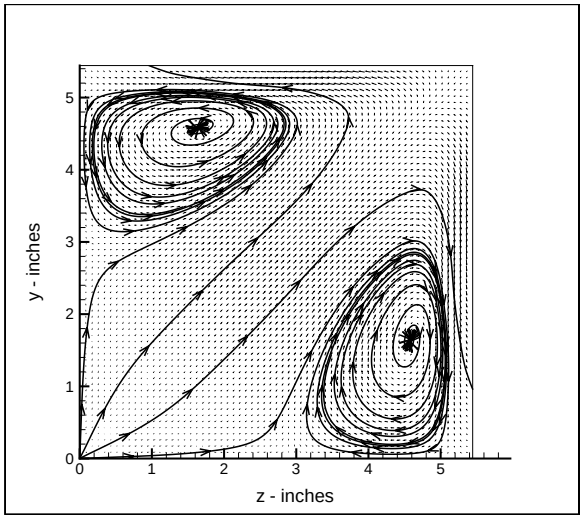

Figure 3: Cross-Flow Velocity Vectors and Streamlines at the Exit of the Square-Cross-Section Nozzle

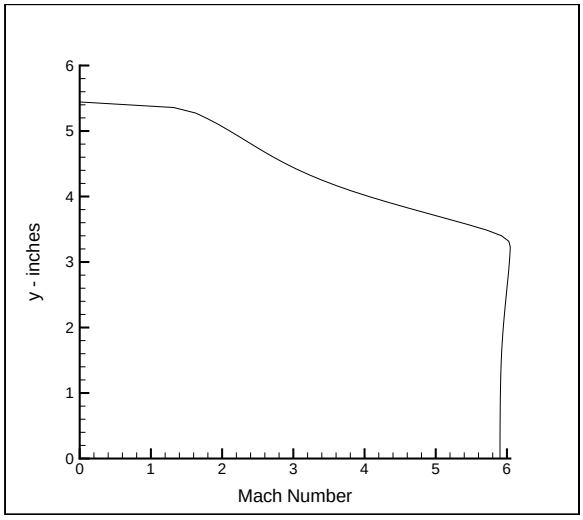

Figure 5: Mach Number Profile at the Square-Cross-Section Nozzle Exit Symmetry Plane

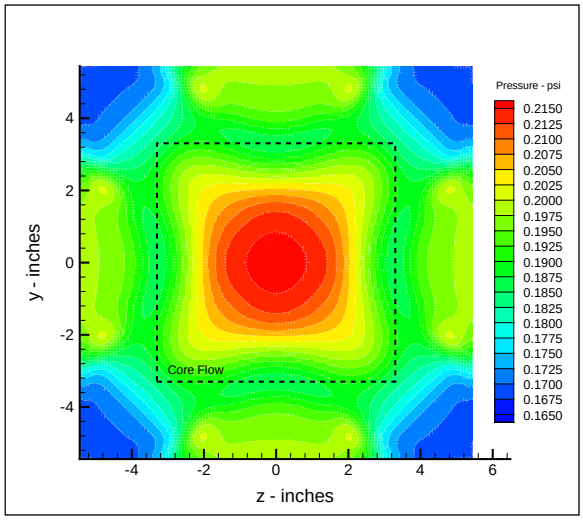

Figure 4: Pressure Contours at the Exit of the Square-Cross-Section Nozzle

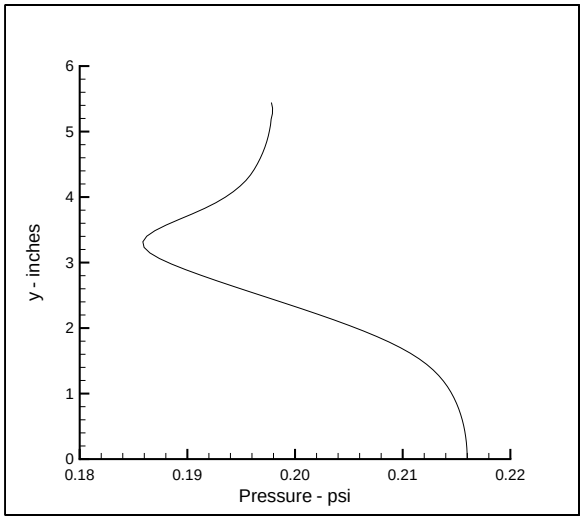

Figure 6: Pressure Profile at the Square-Cross-Section Nozzle Exit Symmetry Plane

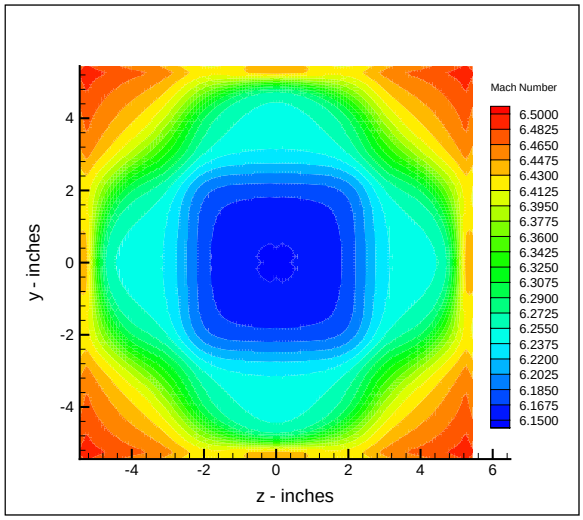

Figure 7: Mach Number Contours at the Square-Cross-Section Nozzle Exit - Inviscid Flow

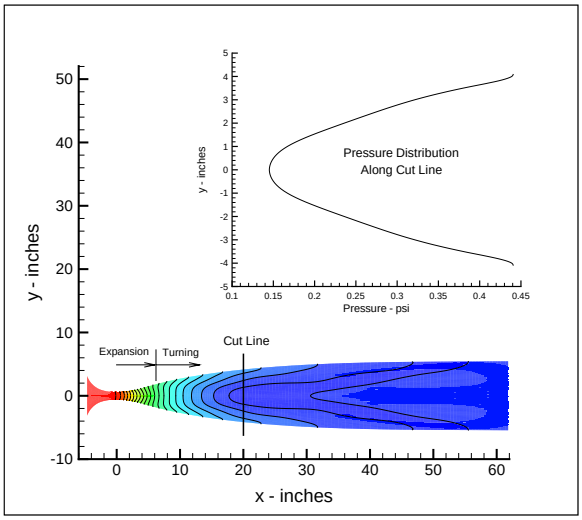

Figure 9: Pressure Variation in the vertical symmetry-plane of the Square-Cross-Section Nozzle

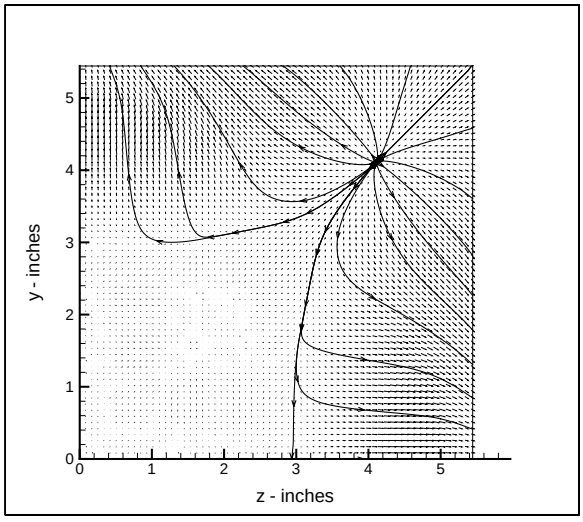

Figure 8: Cross-Flow Velocity Vectors and Streamlines at the Square-Cross-Section Nozzle Exit - Inviscid Flow

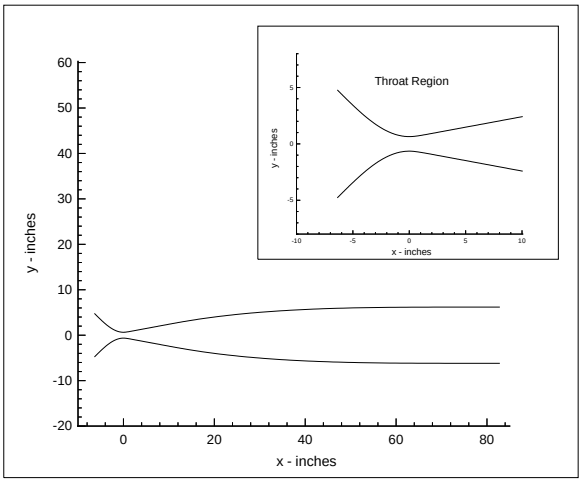

Figure 10: Axisymmetric Nozzle Contour

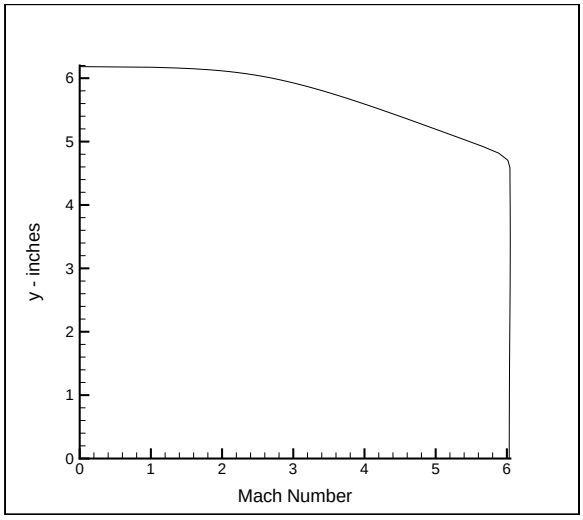

Figure 11: Mach Number Profile at the Exit of the Axisymmetric Nozzle

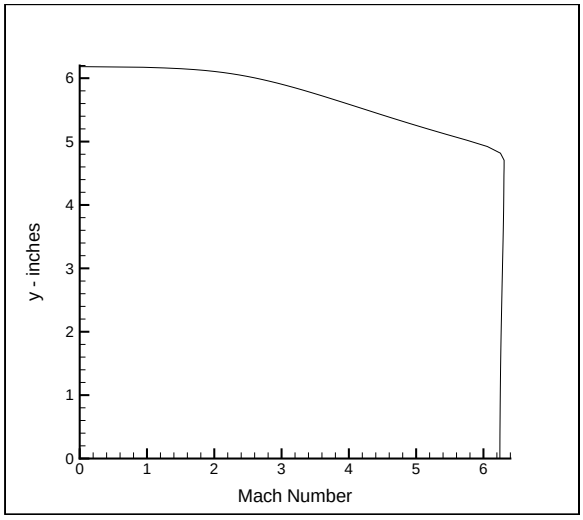

Figure 13: Mach Number Profile at the Exit of the Axisymmetric Nozzle, Mach-5 Flight-Enthalpy

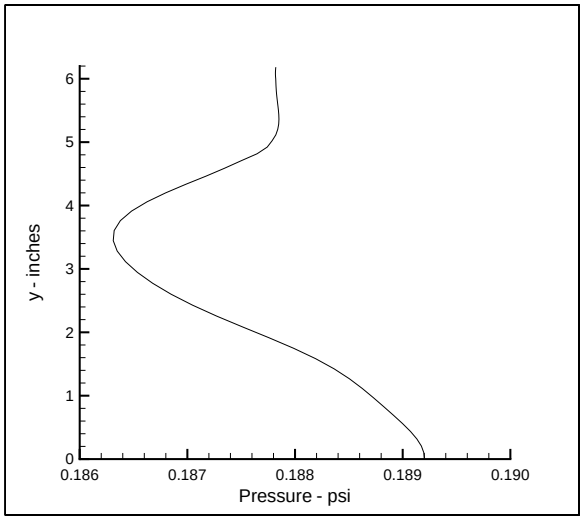

Figure 12: Pressure Profile at the Exit of the Axisymmetric Nozzle

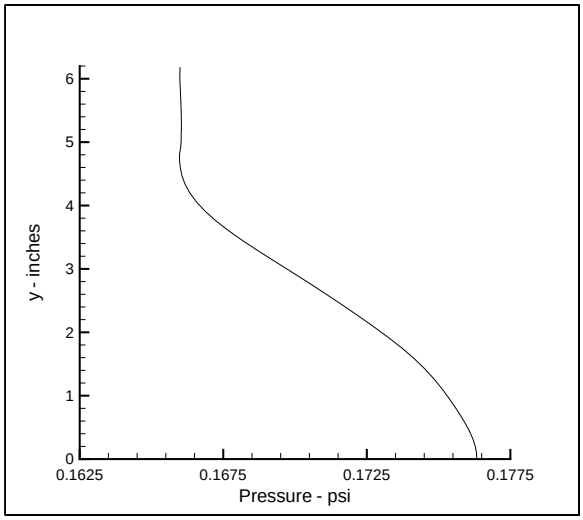

Figure 14: Pressure Profile at the Exit of the Axisymmetric Nozzle, Mach-5 Flight-Enthalpy

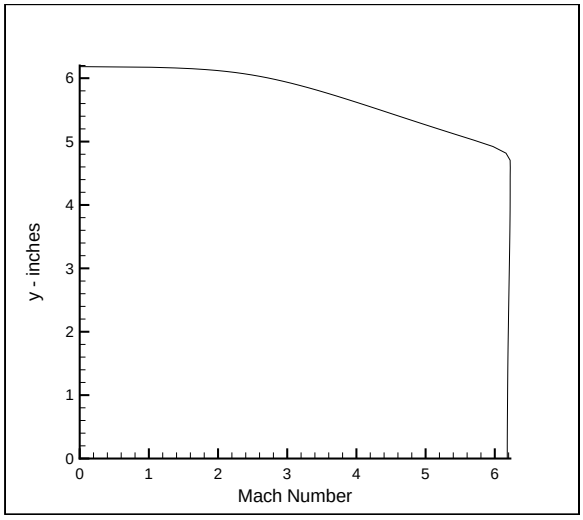

Figure 15: Mach Number Profile at the Exit of the Axisymmetric Nozzle, Mach-6 Flight-Enthalpy

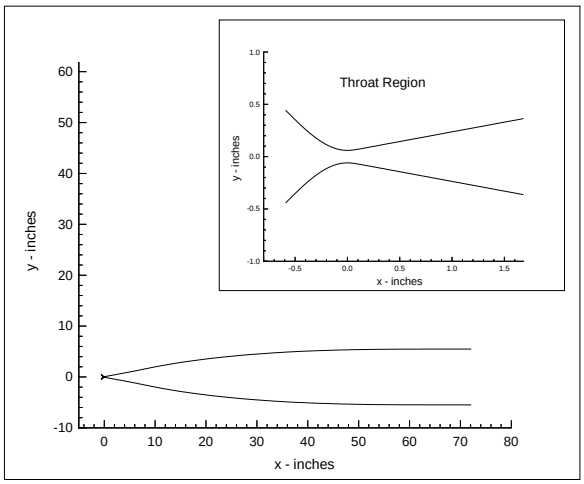

Figure 17: 2-D Nozzle Contour

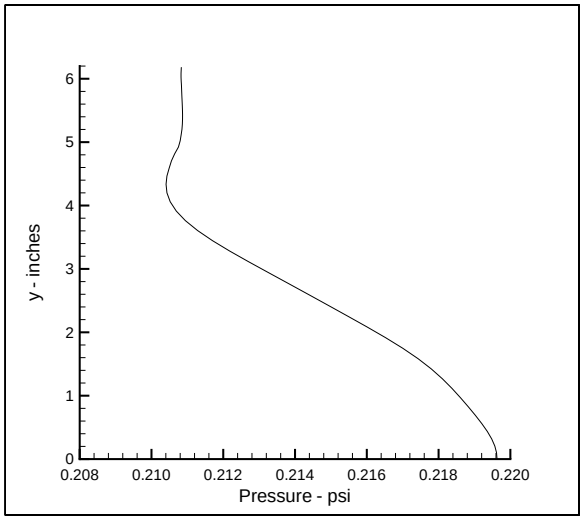

Figure 16: Pressure Profile at the Exit of the Axisymmetric Nozzle, Mach-6 Flight-Enthalpy

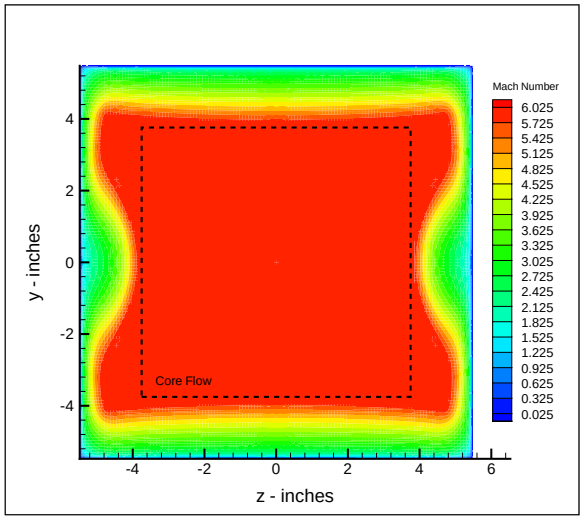

Figure 18: Mach Contours at the 2-D Nozzle Exit

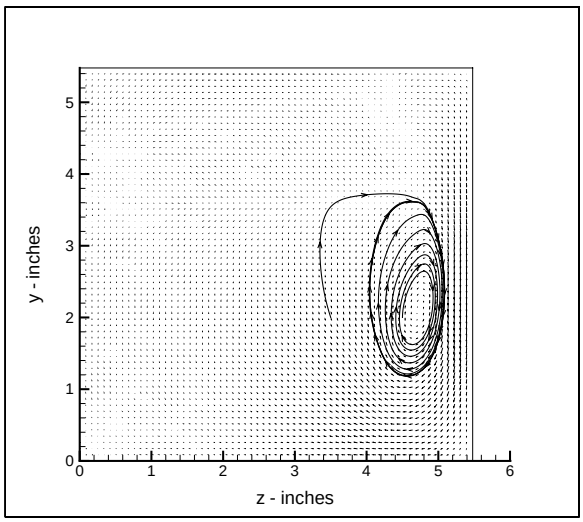

Figure 19: Cross-Flow Velocity Vectors and Streamlines at the 2-D Nozzle Exit

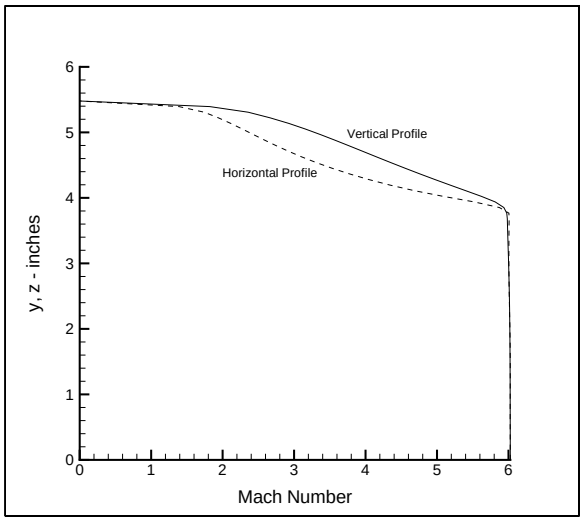

Figure 21: Mach Number Profiles at the 2-D Nozzle Exit (Horizontal and Vertical symmetry planes)

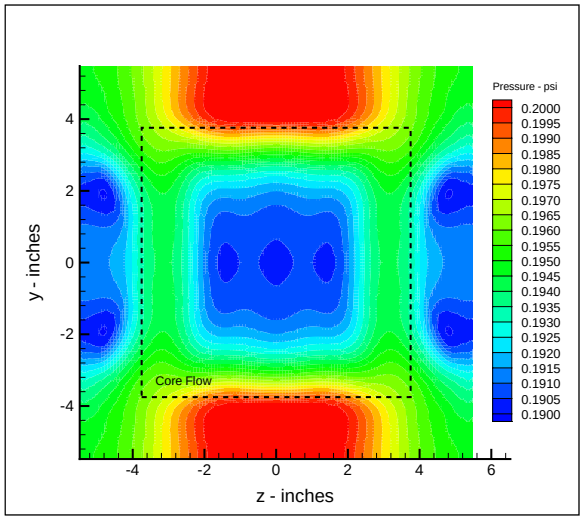

Figure 20: Pressure Contours at the 2-D Nozzle Exit

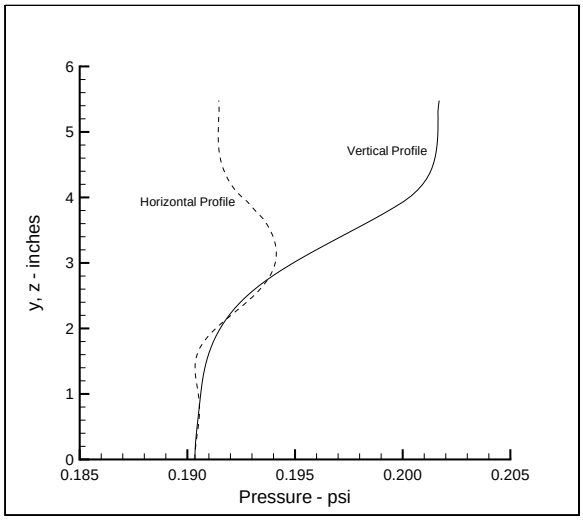

Figure 22: Pressure Profiles at the 2-D Nozzle Exit (Horizontal and Vertical symmetry planes)

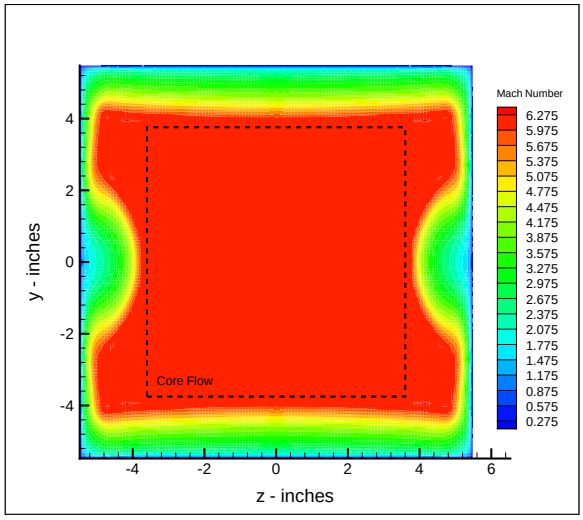

Figure 23: Mach Contours at the 2-D Nozzle Exit, Mach-5 Flight-Enthalpy

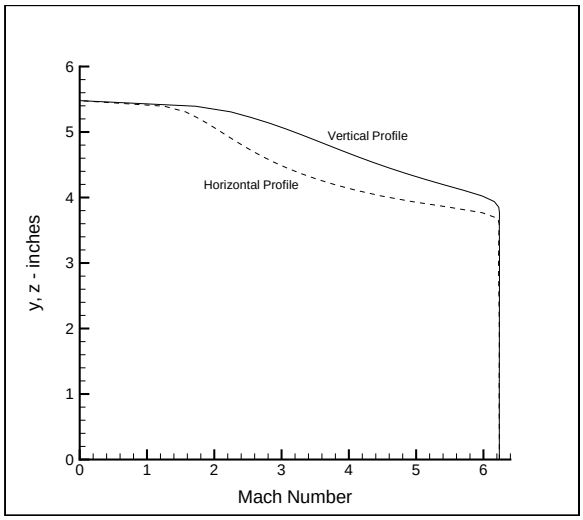

Figure 25: Mach Number Profiles at the 2-D Nozzle Exit (Horizontal and Vertical symmetry planes), Mach-5 Flight-Enthalpy

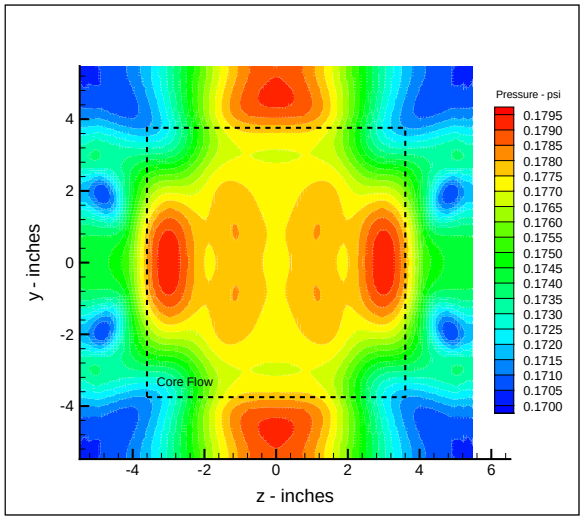

Figure 24: Pressure Contours at the 2-D Nozzle Exit, Mach-5 Flight-Enthalpy

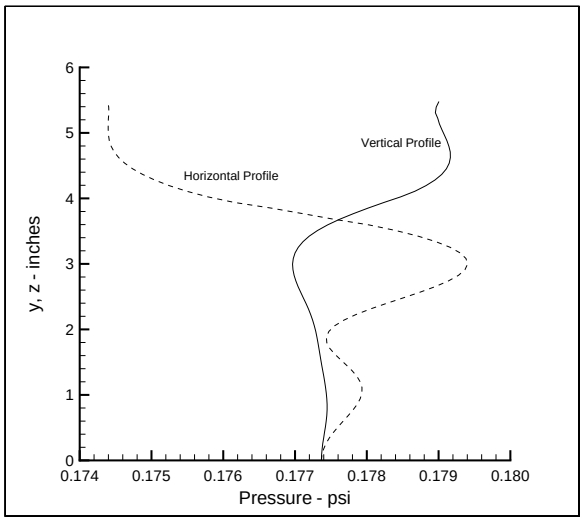

Figure 26: Pressure Profiles at the 2-D Nozzle Exit (Horizontal and Vertical symmetry planes), Mach-5 Flight-Enthalpy

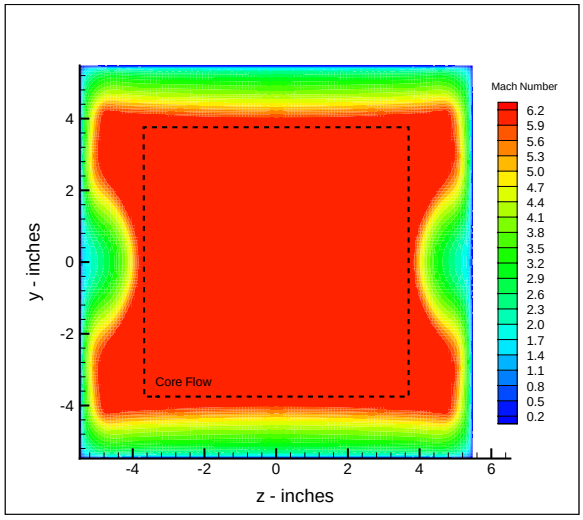

Figure 27: Mach Contours at the 2-D Nozzle Exit, Mach-6 Flight-Enthalpy

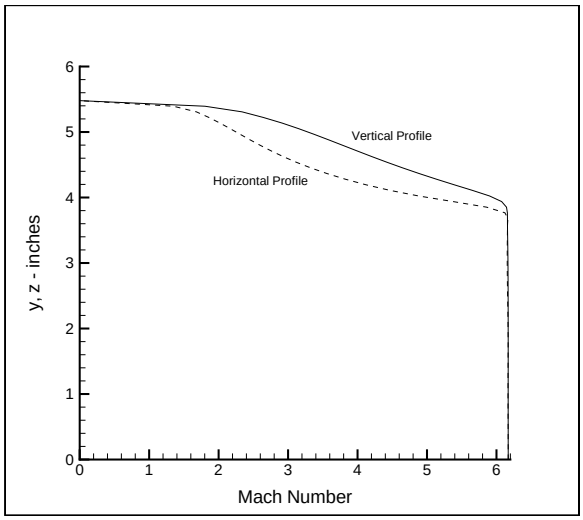

Figure 29: Mach Number Profiles at the 2-D Nozzle Exit (Horizontal and Vertical symmetry planes), Mach-6 Flight-Enthalpy

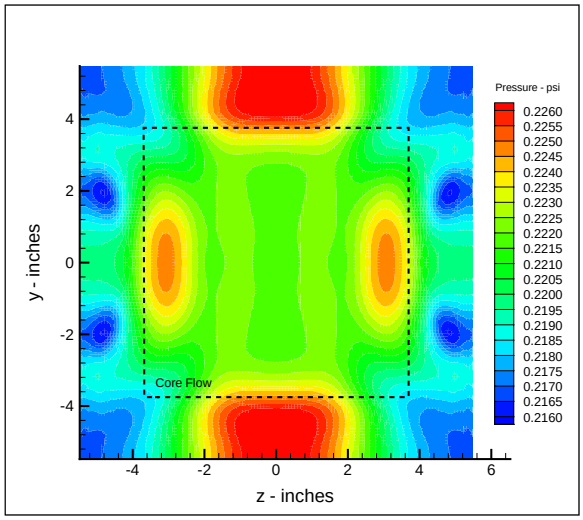

Figure 28: Pressure Contours at the 2-D Nozzle Exit, Mach-6 Flight-Enthalpy

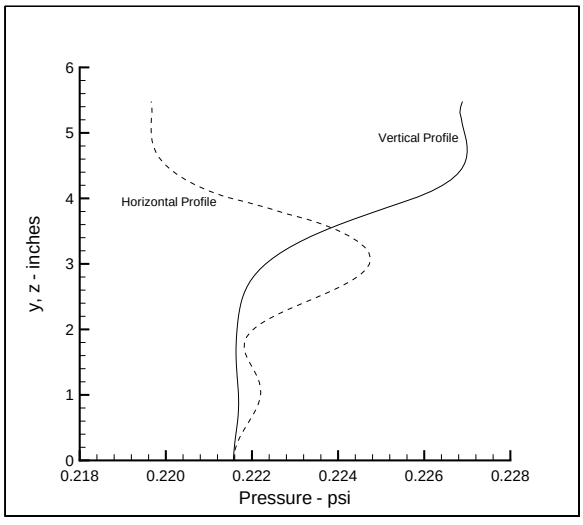

Figure 30: Pressure Profiles at the 2-D Nozzle Exit (Horizontal and Vertical symmetry planes), Mach-6 Flight-Enthalpy

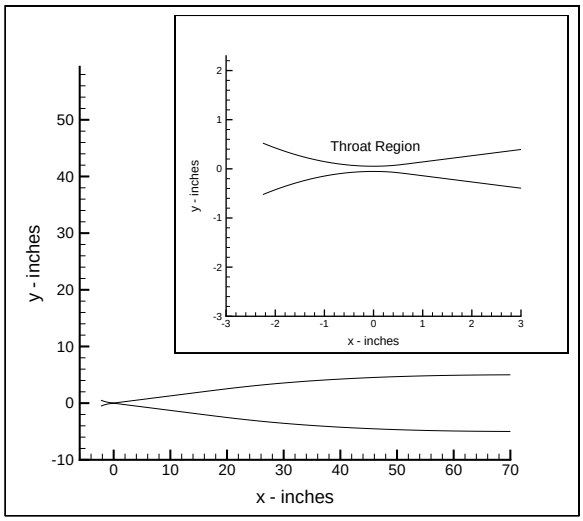

Figure 31: New Mach-6 Nozzle Contour

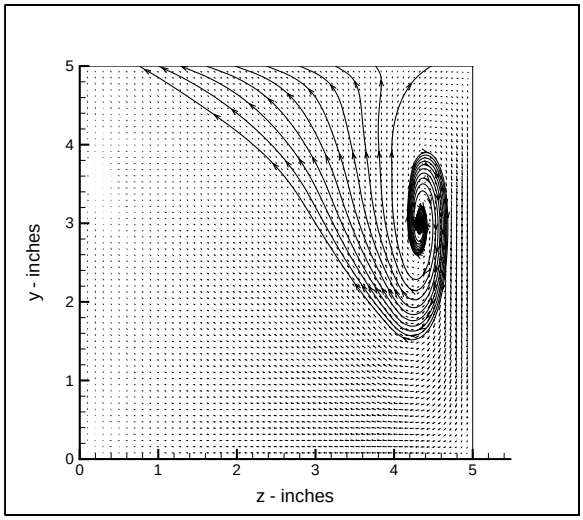

Figure 33: Cross-Flow Velocity vectors and Streamlines in the Exit Plane of the New Mach-6 Nozzle

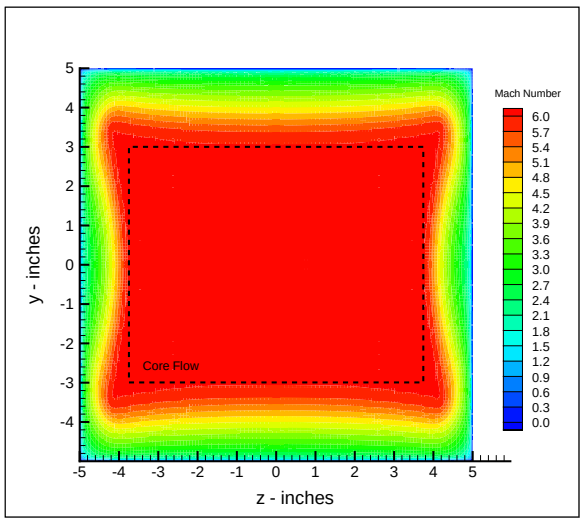

Figure 32: Mach Contours in the Exit Plane of the New Mach-6 Nozzle

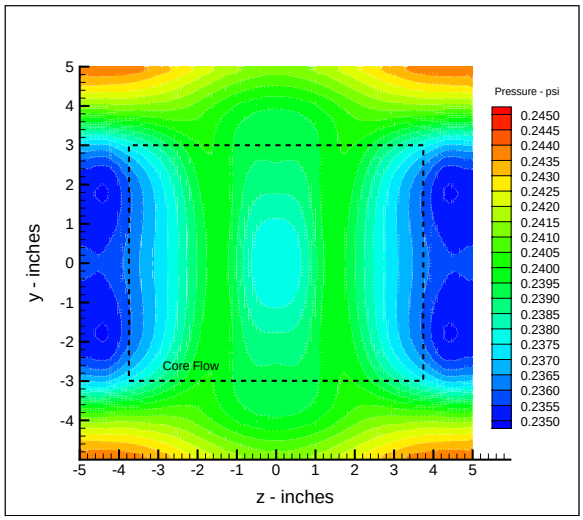

Figure 34: Pressure Contours in the Exit Plane of the New Mach-6 Nozzle

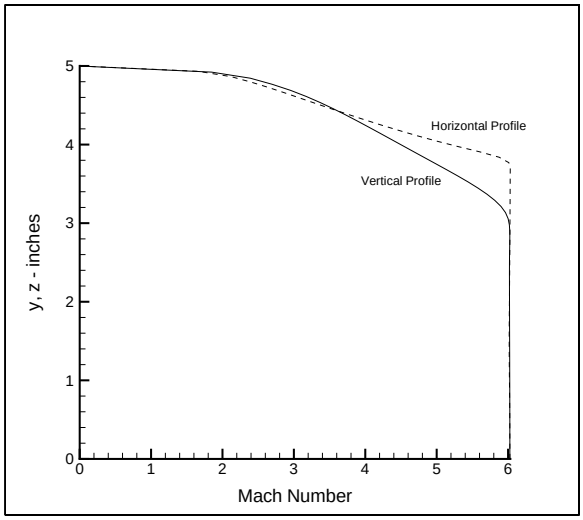

Figure 35: Mach Number Profiles in Vertical and Horizontal Lines at the Exit of the New Mach-6 Nozzle

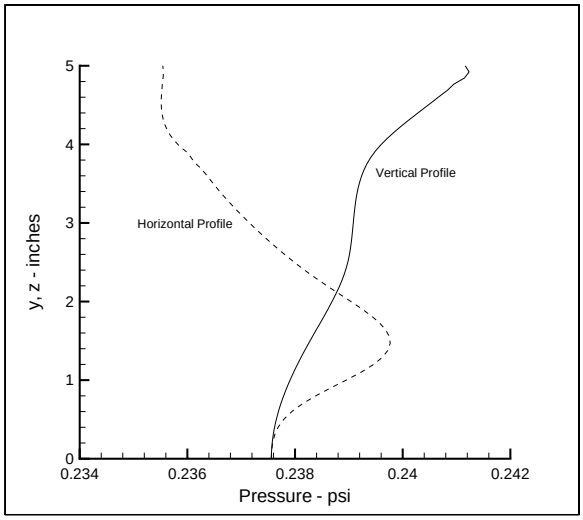

Figure 36: Pressure Profiles in Vertical and Horizontal Lines at the Exit of the New Mach-6 Nozzle